J. Shanghai Jiao Tong Univ. (Sci.), 2021, 26(6): 819-827
https://doi.org/10.1007/s12204-020-2242-8

Parameter Identification of Structural Nonlinearity by Using Response Surface Plotting Technique

LIU Xin[1*] (刘　鑫), *WANG Lixiao*[1] (王力晓), *CHEN Qidong*[1] (陈启东), *SUN Beibei*[2] (孙蓓蓓)
(1. School of Mechanical Engineering, Changshu Institute of Technology, Changshu 215500, Jiangsu, China;
2. School of Mechanical Engineering, Southeast University, Nanjing 211189, China)

Abstract: With rigorous dynamic performance of mechanical products, it is important to identify dynamic parameters exactly. In this paper, a response surface plotting method is proposed and it can be applied to identify the dynamic parameters of some nonlinear systems. The method is based on the principle of harmonic balance method (HBM). The nonlinear vibration system behaves linearly under the steady-state response amplitude, which presents the equivalent stiffness and damping coefficient. The response surface plot is over two-dimensional space, which utilizes excitation as the vertical axis and the frequency as the horizontal axis. It can be applied to observe the output vibration response data. The modal parameters are identified by the response surface plot as linearity for different excitation levels, and they are converted into equivalent stiffness and damping coefficient for each resonant response. Finally, the HBM with first-order expansion is utilized for identification of stiffness and damping coefficient of nonlinear systems. The classical nonlinear systems are applied in the numerical simulation as the example, which is used to verify its effectiveness and accuracy. An application of this technique for nonlinearity identification by experimental setup is also illustrated.
Key words: structural nonlinearity, parameter identification, equivalent stiffness and damping, response surface plot
CLC number: TH 113.1　　**Document code:** A

0 Introduction

Most practical assembled structures do not comply with an assumption of linearity, and the difficulty of modeling mainly is caused by less understanding of structural nonlinearity[1-5]. Frictional contact and micro-slip within assembled structures would introduce complex nonlinearities into mechanical products. Dynamic analysis has highlighted the importance of nonlinearity identification, and the nonlinear effects can not be neglected[6-7]. The investigation of nonlinear mechanism within mechanical products has become an important research field[8]. So it is necessary to identify structural nonlinearity and predict output vibration response during product design stage.

It needs to develop a new technique to extract nonlinear element. Vibration test is necessary for nonlinearity identification and mathematical model update. Mathematical model not only needs to represent physical merits, but also to predict its dynamic response exactly. Some promising methods show fairly satisfactory results. Prawin et al.[9] presented a new technique based on null subspace analysis for detection of nonlinearity, and the structural nonlinearity could be estimated by using ambient vibration data. Effectiveness of the proposed approach was demonstrated by using carefully designed numerical examples. Noël et al.[10] identified a real aerospace structure with strong nonlinearity, which included typical jumps, modal interactions, force relaxation and chattering during impacts. Alejo et al.[11] developed an experimental identification method based on frequency response function (FRF) decoupling and optimization algorithm to model bolted joint interface. It is easy to obtain the FRF in the vibration test procedure, so frequency domain techniques are more advantageous. Göge et al.[12] utilized the linear plotting method to aircraft experimentally. The method can be implemented on large scale structures, but it is only used for detection of nonlinearities rather than quantification. Sadati et al.[13] introduced an optimum equivalent linear frequency response function (OELF) to identify dynamic parameters of nonlinear joint. The OELF method has the advantage of using standard vibration tests, but it is restricted to complicated iterative procedures. The linearization method was improved by Özer et al.[14]. Sherman-Morrison inversion was used to obtain equivalent stiffness and damping dependent of response amplitude, and the values of equivalent stiffness and damping were calculated at different excitation frequency. Feldman and Braun[15] dealt with the identification of nonlinear vibration systems based

Received: 2019-04-16　　**Accepted:** 2019-07-16
*__E-mail:__ liuxin2174897@163.com

on measured signals for free and forced vibration regimes via Hilbert decomposition. Different identification methods based on experimental procedure have their own advantages and drawbacks.

In this study, response surface plot is developed to identify nonlinear parameters by experimental data in frequency-domain. Numerical and experimental analyses are applied for simulation. The identification method mainly depends on the basic idea that non-linear structures exhibit linear behavior under steady response amplitude[9-14]. Equivalent stiffness and damping coefficient can be obtained for each excitation level. The accurate stiffness and damping function of response amplitude are constructed by fitting, which is used to describe nonlinear behavior for nonlinear identification by harmonic balance method (HBM).

1 Response Surface Plot

1.1 Equivalent Stiffness and Damping

If the dynamic behavior of engineering structures is an isolated nonlinear mode, the governing equation of a nonlinear system can be expressed as

$$m\ddot{x} + c\dot{x} + kx + n(x, \dot{x}) = f(t), \tag{1}$$

where, m, c and k are the mass, stiffness and damping of the linear part, respectively; x is the response displacement; $f(t)$ is the external force; $n(x, \dot{x})$ is the nonlinear force, which means interior nonlinear spring or damping force. The proposed procedure bases on the idea that most vibration energy is concentrated in the excitation frequency ω, and the vibration response can be regarded as linearity under steady response amplitude[10-12]. If a nonlinear structure is excited by harmonic excitation, the force value is expressed as

$$f(t) = F\mathrm{e}^{\mathrm{i}\omega t}, \tag{2}$$

where, F represents the excitation amplitude; ω is the excitation frequency. The vibration response amplitude can be rewritten as

$$x(t) = X\mathrm{e}^{\mathrm{i}(\omega t+\psi)}, \tag{3}$$

where, X denotes the amplitude; ψ denotes the phase information of response. When Eq. (3) is substituted into nonlinear force $n(x, \dot{x})$, the nonlinear spring and damping element can be presented by linear describing function $k(X)$ or $c(X)$ by HBM with first-order expansion. The application of HBM gives parameters dependent of response and it is regarded as equivalent stiffness and damping[13]. As for generalized nonlinearity, the derivation of equivalent stiffness and damping can be conducted by Eqs. (4) and (5), and nonlinear stiffness and damping are linearized at that specific response amplitude. The equivalent stiffness and damping can be written as $k(X)$ and $c(X)$ as[13-14]

$$k(X) = \frac{1}{\pi X}\int_0^{2\pi} n_k(x)\sin\Phi \mathrm{d}\Phi, \tag{4}$$

$$c(X) = \frac{1}{\pi\omega X}\int_0^{2\pi} n_c(\dot{x})\cos\Phi \mathrm{d}\Phi, \tag{5}$$

where $\Phi = \omega t + \psi$, and $n_k(x)$ and $n_c(\dot{x})$ present the nonlinear spring and damping forces. For the purpose of explanation, classical cubic stiffness will be presented as an example. Considering the motion equation of a linear damped system, Eq. (1) can be given as

$$m\ddot{x} + c\dot{x} + kx + \alpha x^3 = f(t), \tag{6}$$

where α is nonlinear stiffness. The nonlinear force $n(x, \dot{x}) = \alpha x^3$ can be approximated by Fourier expansion with first-order expansion by Eq. (4), and the describing function is presented as

$$k(X) = \frac{3}{4}\alpha X^2, \tag{7}$$

so Eq. (6) can be rewritten as

$$m\ddot{x} + c\dot{x} + \left(k + \frac{3}{4}\alpha X^2\right)x = f(t). \tag{8}$$

Equivalent stiffness varies with response amplitude, and it provides an approximation of nonlinear interior force and presents some equivalent amplitude-dependent modal parameters. From Eq. (8), resonant frequency and damping ratio can be extracted for each steady response as

$$\omega_\mathrm{n}(X) = \sqrt{\left(k + \frac{3}{4}\alpha X^2\right)\Big/ m}, \tag{9}$$

$$\zeta(X) = c\Big/ 2\sqrt{\left(k + \frac{3}{4}\alpha X^2\right)m}. \tag{10}$$

Modal parameters shift with response amplitude according to Eqs. (9) and (10). If the variation of modal parameters with respect to response amplitude is obtained, the nonlinear receptance can be written as

$$H(\omega, X) = \frac{A}{\omega_\mathrm{n}(X)^2 - \omega^2 + 2\mathrm{i}\zeta(X)\omega\omega_\mathrm{n}(X)}, \tag{11}$$

where A is the modal constant of the system. Nonlinear receptance seems linear corresponding to the steady response and generates effectively quasi linear behavior. Harmonic response prediction at desired excitation needs iteration, and convergent value will be considered as the calculation result[16].

1.2 Procedure

As the nonlinear FRF mainly depends on exterior excitation level, it shifts due to inherent nonlinearity[17-19]. If experimental FRFs are measured, vibration response is calculated at different excitation levels. And the vibration response data is plotted against ω and f as discrete points by a repeatable surface. Surface plot can be used for observation of vibration response data for different excitation levels. The resonant frequency $\omega_n(X)$ or damping ratio $\zeta(X)$ shift for different forcing levels when approaching resonances, which provides evolution of resonant frequency and damping ratio with resonant amplitude X. First, it needs to calculate the (modal) mass of the system. Then, the modal quantities need to be converted into spatial quantities. Equivalent stiffness and damping can be obtained for each excitation level corresponding to X. The equivalent stiffness can be obtained by multiplying the (modal) mass extracted from the inverse receptance by the resonant frequency. Equivalent damping can be extracted by using relationship $c(X) = 2\zeta(X)m\omega_n(X)$. Extraction tools may be applied separately for different excitation levels. The equivalent stiffness and damping varies with steady response and can be considered as amplitude-dependent. The discrete stiffness and damping can be fitted as suitable basis function as $k(X)$ and $c(X)$. Fitting results can be employed to characterize the nonlinear element according to stiffness and damping function by HBM with first-order expansion. Equivalent stiffness and damping by standard vibration test and nonlinearity extraction can be carried out for each excitation, which fits the stiffness and damping function to describe nonlinear behavior and identify nonlinearity. The nonlinear parameter identification method is clearly presented by response surface plot procedure as shown in Fig. 1.

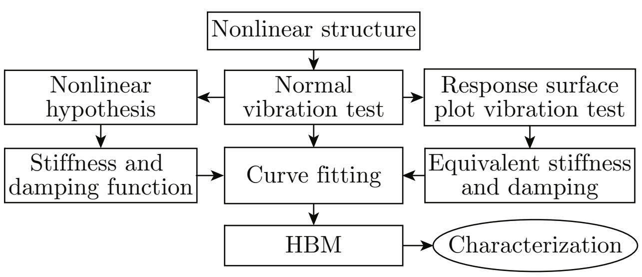

Fig. 1 Flowchart of nonlinear parameter identification by response surface plot

2 Application to Numerical Case Study

Typical nonlinear numerical models are applied to validate the procedure by simulation process. It is used for nonlinear parameter identification. The purpose is to show its application by numerical analysis. The governing equation of the dynamic response of the system is presented as

$$m\ddot{x} + c\dot{x} + kx + n_k(x) + n_c(\dot{x}) = f(t). \quad (12)$$

The solution of the nonlinear motion system is calculated by using a Runge-Kutta method ode45 in MATLAB software. The time-domain response lasts for enough time to ensure a steady-state response that is required. The important frequency is chosen as the excitation frequency. Utilizing the response and excitation data and transforming them into frequency by fast fourier transform (FFT), the response surface plot is obtained against ω and f for calculating the equivalent stiffness and damping.

2.1 Cubic Stiffness

Classical Duffing oscillator is classical polynomial stiffness, which is usually used to describe nonlinearity for engineering structures. The nonlinear spring force $k_{n1}x^3$ is presented by

$$m\ddot{x} + c_1\dot{x} + k_1x + k_{n1}x^3 = f(t). \quad (13)$$

The equivalent stiffness function is

$$k(X) = k_1 + \frac{3}{4}k_{n1}X^2, \quad (14)$$

where k_{n1} is the cubic stiffness. If $k_{n1} > 0$, it is hardening. If $k_{n1} < 0$, it is softening. The response surface plot for softening cubic stiffness is shown in Fig. 2. It can be observed that the shift of peak response frequency is obvious with increasing excitation level. The resonant frequency dwindles simultaneously with response amplitude in Fig. 3. Equivalent stiffness (k) is obtained according to the procedure in Section 1.2, and a consistent decrease of equivalent stiffness is observed by a quadratic law in Fig. 4(a). The equivalent stiffness reveals underlying linear characteristic and the linear equivalent damping (c) can be seen in Fig. 4(b).

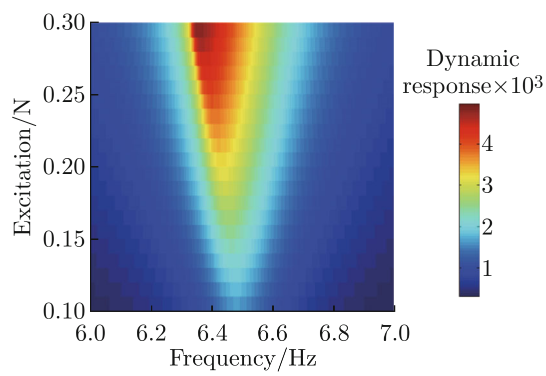

Fig. 2 Response surface plot for cubic stiffness

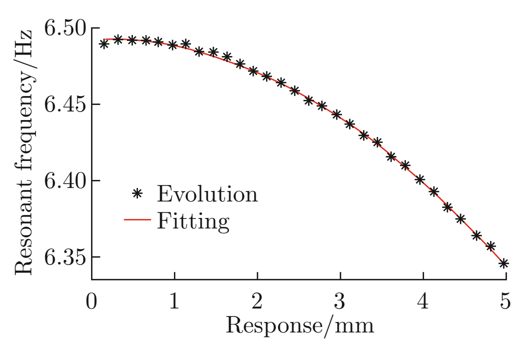

Fig. 3 Evolution of resonant frequency for cubic stiffness

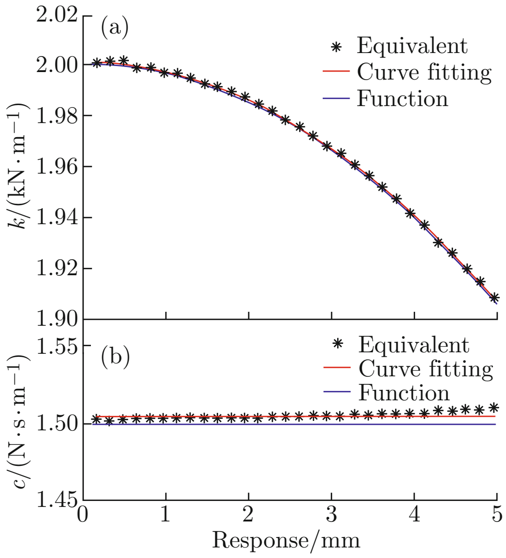

Fig. 4 Identification for cubic stiffness

2.2 Quintic Stiffness

The quintic stiffness with hardening nonlinearity is

$$m\ddot{x} + c_2\dot{x} + k_2x + k_{n2}x^5 = f(t), \tag{15}$$

where k_{n2} is the nonlinear quintic stiffness. According to Eq. (4), the equivalent stiffness is obtained as

$$k(X) = k_2 + \frac{5}{8}k_{n2}X^4. \tag{16}$$

The increase of resonant frequency can be observed by the response surface plot in Fig. 5, which shows hardening polynomial stiffness via resonant frequency shift trend. It is seen from Eq. (16) that equivalent stiffness increases with the response level. It is proportional to displacement amplitude to the fourth power by equivalent linearity plot in Fig. 6(a). The linear damping can be seen in Fig. 6(b).

2.3 Coulomb Damping

The Coulomb damping model is a type of static friction model. It affects significantly if the excitation level is not very high. The plot in Fig. 7 is the simulated

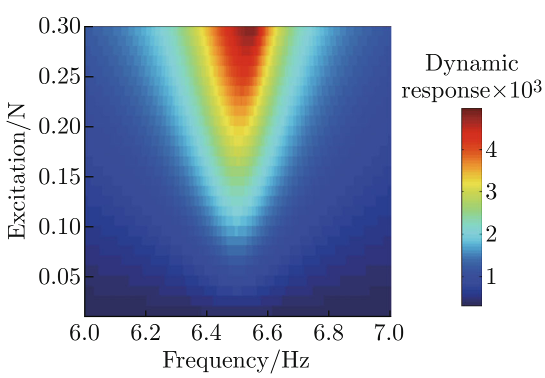

Fig. 5 Response surface plot for quintic stiffness

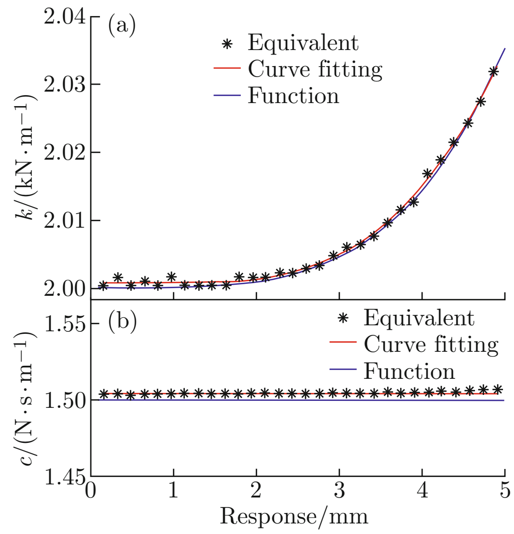

Fig. 6 Identification for quintic stiffness

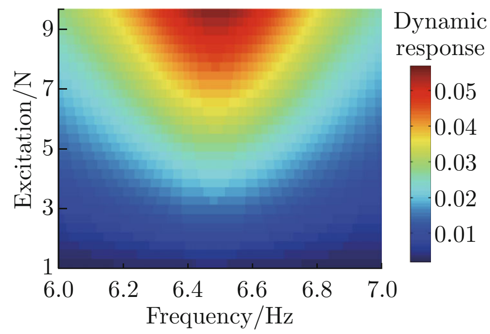

Fig. 7 Response surface plot for Coulomb damping

result of vibration response data considering Coulomb friction.

$$m\ddot{x} + c_3\dot{x} + k_3x + F_f\mathrm{sgn}(\dot{x}) = f(t), \tag{17}$$

where F_f is the friction force. The equivalent damping of Coulomb damping can be defined as according to Eq. (5):

$$c(X) = c_3 + \frac{4F_f}{\pi\omega x}. \tag{18}$$

The linear stiffness is plotted in Fig. 8(a). The significant decrease in damping with hyperbolic trend especially for small response amplitude is an indication of Coulomb damping shown in Fig. 8(b).

2.4 Piecewise Stiffness

Piecewise stiffness is the combination of linear stiffness, which shows different stiffness for different response amplitudes. Its spring characteristic can be seen by

$$\left.\begin{aligned} &m\ddot{x} + c_4\dot{x} + k_5x + (k_4 - k_5)b = f(t), && x > b \\ &m\ddot{x} + c_4\dot{x} + k_4x = f(t), && |x| \leqslant b \\ &m\ddot{x} + c_4\dot{x} + k_5x - (k_4 - k_5)b = f(t), && x < -b \end{aligned}\right\}, \tag{19}$$

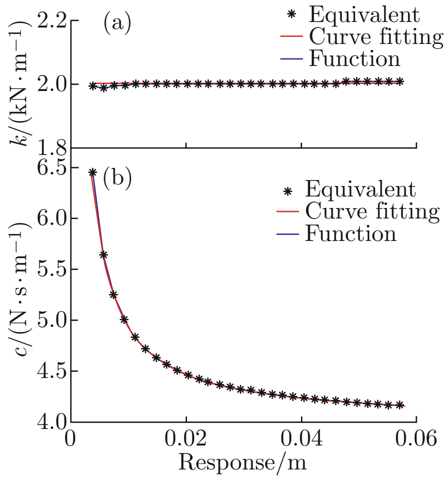

Fig. 8 Identification for Coulomb damping

where b is the transition point of piecewise stiffness. sAnd its equivalent stiffness is obtained by Eq. (4):

$$k(X) = k_5 - \frac{k_5 - k_4}{\pi}\left[2\sin^{-1}\left(\frac{b}{x}\right) + \frac{b}{x^2}\sqrt{x^2 - b^2}\right]. \quad (20)$$

The piece stiffness can be observed by the plot in Fig. 9. A small shift of resonant frequency occurs for the case of piecewise stiffness in comparison with polynomial stiffness. When the excitation level is low, it behaves linearly. And the resonant frequency is consistent as stiffness value is k_4. With the increase of excitation level, the response amplitude is close to the region of stiffness k_5 and the system becomes nonlinear. The transition of stiffness from k_4 to k_5 occurs that can be seen in Fig. 10.

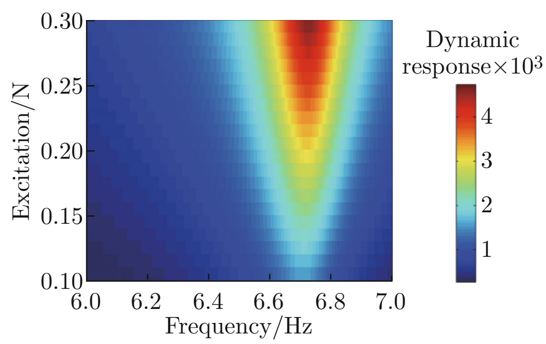

Fig. 9 Response surface plot for piecewise stiffness

2.5 Bilinear Stiffness

The stiffness is changed at the zero point for bilinear stiffness. For the positive displacement, the stiffness is k_6; while for the negative displacement, the stiffness is k_7.

$$\left.\begin{array}{ll} m\ddot{x} + c_5\dot{x} + k_6 x = f(t), & x > 0 \\ m\ddot{x} + c_5\dot{x} + k_7 x = f(t), & x < 0 \end{array}\right\}. \quad (21)$$

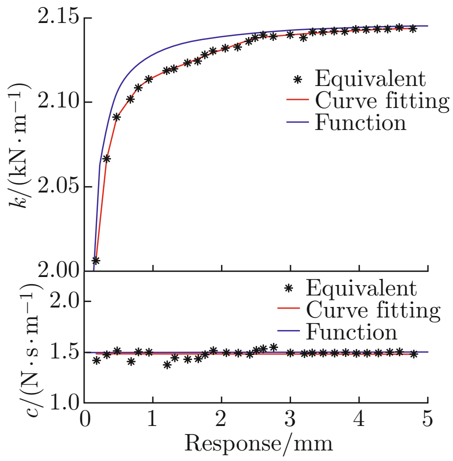

Fig. 10 Identification for piecewise stiffness

The equivalent stiffness of the system is

$$k(X) = \frac{k_6 + k_7}{2}. \quad (22)$$

The surface plot of bilinear stiffness can be seen in Fig. 11. It shows that the amplitude-dependent resonant frequency is nearly a constant, and there is no change for the equivalent stiffness with increasing response amplitudes. But the nonlinear behavior can be observed in the time-domain response, since the positive response amplitude is lower than the negative response amplitude seen in Fig. 11(d). And the stiffness k_6 and k_7 can be obtained according to the positive and negative responses.

2.6 Combined Nonlinearity

Some real structures usually have combined nonlinearity for industrial application. Quadratic damping is the most common polynomial damping and the equivalent damping of quadratic damping $c\dot{x} + c_n\dot{x}|\dot{x}|$ is

$$c(X) = c + \frac{8c_n V}{3\pi}, \quad (23)$$

where, c_n is the nonlinear damping; $V + X\omega$ is the velocity amplitude. Two different types of non-linearities are considered simultaneously as

$$m\ddot{x} + c_6\dot{x} + c_{n6}\dot{x}|\dot{x}| + k_8 x + k_{n8}x^3 = f(t). \quad (24)$$

3 Identification Results and Experimental Study

The stiffness and damping function of response amplitude of combined nonlinearities system is shown in Fig. 12. The good match between equivalent stiffness/damping and the fitted curve as a function of response is shown as above. From these cases, it can be clearly sure that response surface plotting technique adopted in this paper introduces a desired accuracy for nonlinearity characterization. It is based on the assumption that it responds at the same frequency as the excitation. And the equivalent stiffness or damping is

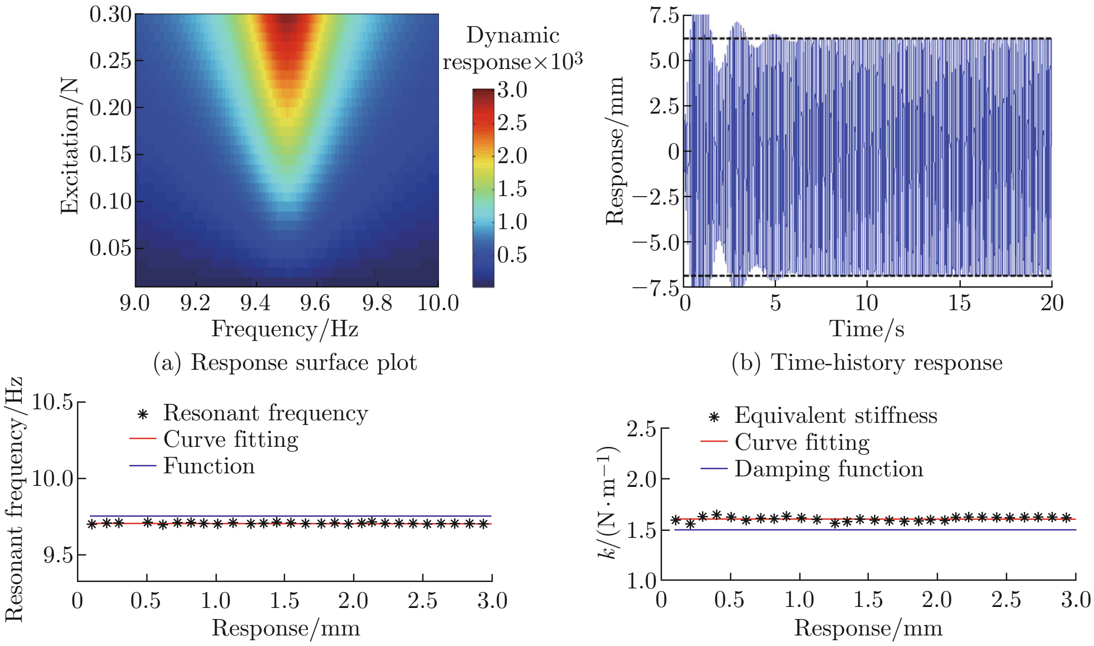

(a) Response surface plot (b) Time-history response

(b) Evolution of resonant frequency (d) Linear stiffness

Fig. 11 Identification for bilinear stiffness

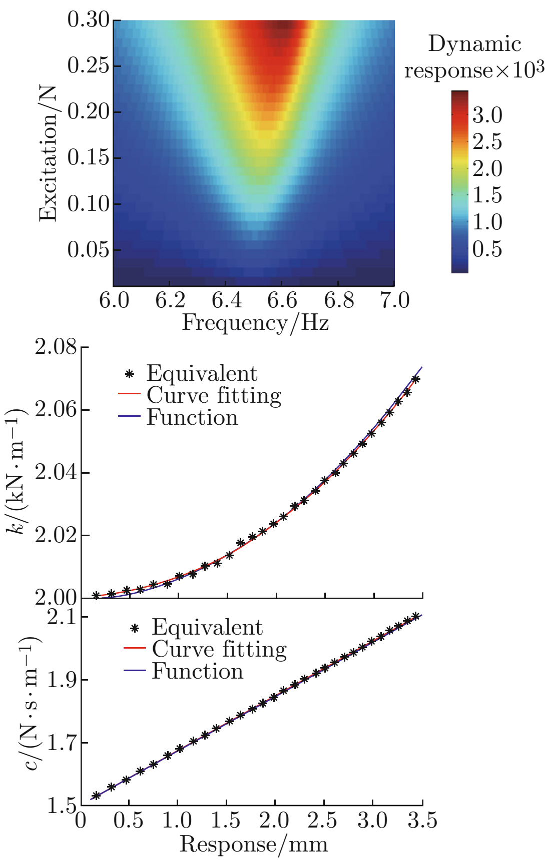

Fig. 12 Identification for combined nonlinearity

similar to HBM with first-order expansion. According to the numerical results, parameter identification for different numerical models can be obtained in Table 1, which reveals that it is able to identify the nonlinear stiffness and damping with small relative error.

The basic procedure of this method has already been verified with classical nonlinear case studies numerically. The application of response surface plotting method is demonstrated by experimental setup. The mechanical joint has a significant influence on the dynamics of assembly and introduces an uncertain nonlinearity along the mechanical joints. Experimental application for nonlinear identification begins with the construction of specimen with 6.2 kg, which is used as a counterweight before. The experimental setup is shown in Fig. 13. The specimen rests on a cushion by four mechanical joints with fixed boundary condition. The concentrated mass is excited by external force by an electromagnetic shaker, which exerts sine-sweep excitations. Because the shaker can regulate the excitation levels and frequency range as needed easily, the attachment point of the force bar stinger is located at the

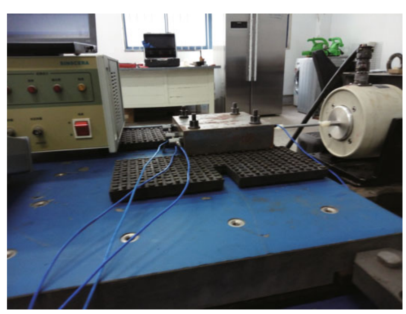
Fig. 13 Experimental setup

Table 1 Identification results and its relative error

Nonlinear type		Parameter value	Identification	Error/%
Cubic stiffness	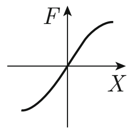	$k_1 = 2\,000\,\mathrm{N/m}$ $c_1 = 1.5\,\mathrm{N\cdot s/m}$ $k_{n1} = -5\times10^6\,\mathrm{N/m^3}$	$k_1 = 2\,001.9\,\mathrm{N/m}$ $c_1 = 1.505\,\mathrm{N\cdot s/m}$ $k_{n1} = -4.930\times10^6\,\mathrm{N/m^3}$	0.095 0.3 1.4
Quintic stiffness	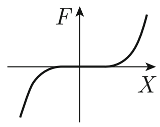	$k_2 = 2\,000\,\mathrm{N/m}$ $c_2 = 1.5\,\mathrm{N\cdot s/m}$ $k_{n2} = 9\times10^{10}\,\mathrm{N/m^5}$	$k_2 = 2\,001.9\,\mathrm{N/m}$ $c_2 = 1.504\,\mathrm{N\cdot s/m}$ $k_{n2} = 8.914\times10^{10}\,\mathrm{N/m^5}$	0.06 0.26 0.95
Coulomb damping	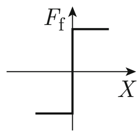	$k_3 = 2\,000\,\mathrm{N/m}$ $c_3 = 4\,\mathrm{N\cdot s/m}$ $F_f = 0.3\,\mathrm{N}$	$k_3 = 2\,001.7\,\mathrm{N/m}$ $c_3 = 4.18\,\mathrm{N\cdot s/m}$ $F_f = 0.286\,\mathrm{N}$	0.085 4.5 4.3
Piecewise stiffness	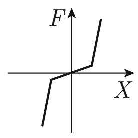	$k_4 = 2\,000\,\mathrm{N/m}$ $k_5 = 2\,150\,\mathrm{N/m}$ $c_4 = 1.5\,\mathrm{N\cdot s/m}$	$k_4 = 2\,010.7\,\mathrm{N/m}$ $k_5 = 2\,142.1\,\mathrm{N/m}$ $c_4 = 1.47\,\mathrm{N\cdot s/m}$	0.54 0.35 2
Bilinear stiffness	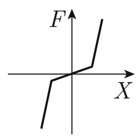	$k_6 = 4\,000\,\mathrm{N/m}$ $k_7 = 5\,000\,\mathrm{N/m}$ $c_5 = 1.5\,\mathrm{N\cdot s/m}$	$k_6 = 4\,081\,\mathrm{N/m}$ $k_7 = 5\,144\,\mathrm{N/m}$ $c_5 = 1.61\,\mathrm{N\cdot s/m}$	2.0 2.8 7.3
Combined nonlinearity	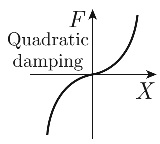	$k_8 = 2\,000\,\mathrm{N/m}$ $k_{n8} = 8\times10^6\,\mathrm{N/m^3}$ $c_6 = 1.5\,\mathrm{N\cdot s/m}$ $c_{n6} = 5\,\mathrm{N\cdot s^2/m^2}$	$k_8 = 2\,001.2\,\mathrm{N/m}$ $k_{n8} = 7.72\times10^6\,\mathrm{N/m^3}$ $c_6 = 1.52\,\mathrm{N\cdot s/m}$ $c_{n6} = 5.013\,\mathrm{N^2\cdot s^2/m^2}$	0.06 3.44 1.3 0.25

input point. And the dynamic response of mass is measured by printed circuit board (PCB) acceleration sensor. All the measurements and excitation are measured by M+P data pickup in the horizontal direction. The first mode is the rigid in the horizontal direction.

It can be seen from Fig. 14 that the first resonant frequency is around 50.4 Hz, which is well separated from other resonances. The middle point is marked by 2 as the excitation point, and the left and right response points are marked by 2 and 3. The obtained

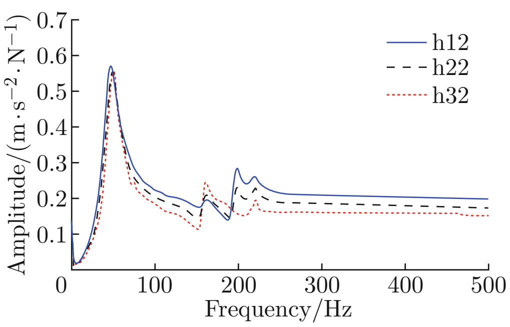

Fig. 14 Measured FRF data in the horizontal direction of 3 accelerometers

FRFs (h12, h22, and h32) also prove that the system dynamic is dominated by the first mode only. As the three 'FRFs' are close to each other according to three accelerators' output, it proves that the first mode is the system in the horizontal direction. This section will introduce the identification of nonlinearity by experimental setup. Sine-sweep vibration test is utilized, and the excitation frequency is chosen to vary close to the first natural mode. The excitation amplitude is maintained at a constant level for frequency range, and the steady-state response of the mass and its corresponding force signal are recorded. And the output of vibration response is obtained. The response surface plot to extract linear and nonlinear behaviors will be presented in Fig. 14. It can be seen from Fig. 15 that the resonant frequency shifts to the left side, which reveals a softening nonlinear stiffness.

$$n_k(x) = 7.244\times10^5 x - 1.1770\times10^{10} x|x| + 1.7613\times10^{14} x^3 - 1.4568\times10^{18} x^3|x| + 4.697\times10^{21} x^5, \quad (25)$$

$$n_c(\dot{x}) = 322\dot{x} + 7.8791\times10^4 \dot{x}|\dot{x}| - 4.3747\times10^6 \dot{x}^3 + 7.6782\times10^7 \dot{x}^3|\dot{x}|. \quad (26)$$

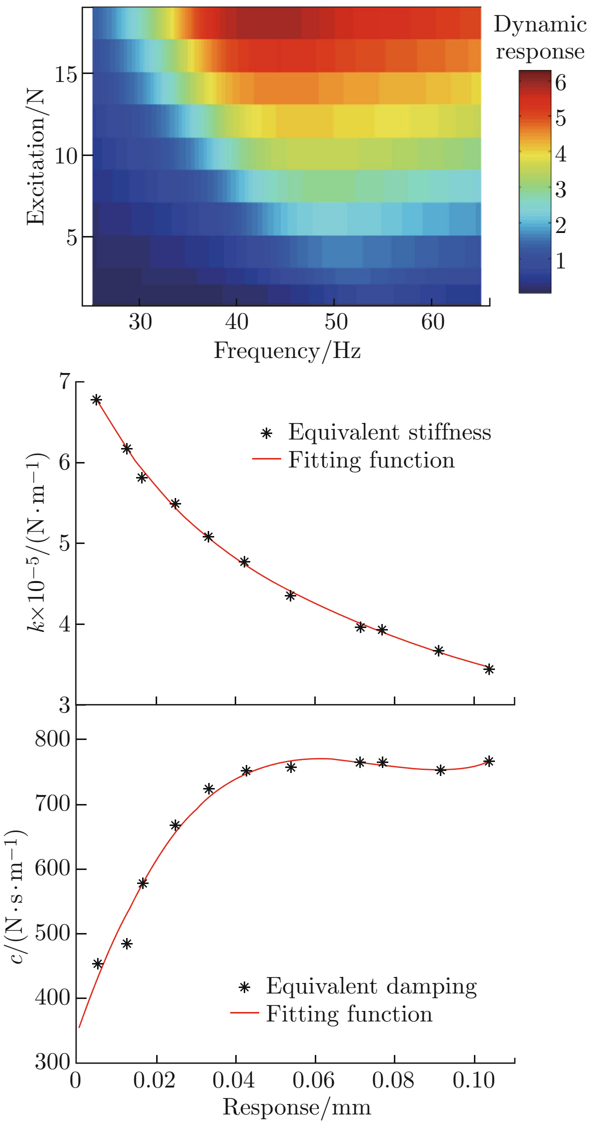

Fig. 15 Identification for experimental setup

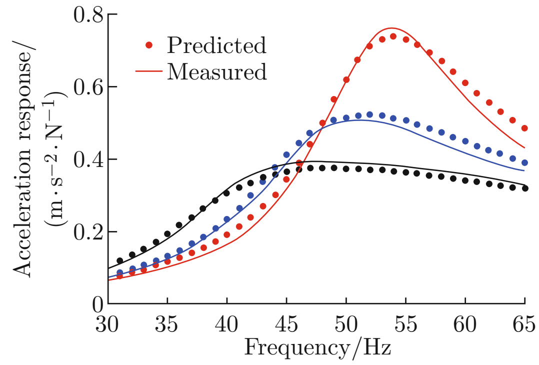

Fig. 16 Comparison between measured and predicted responses for $F = 1, 3, 9\,\mathrm{N}$

The fitting function of response can be approximated in terms of ordinary orthogonal polynomials for the non-smooth nonlinearity seen in Fig. 15, and the nonlinear stiffness and damping forces can be calculated by HBM. Equations (25) and (26) are the stiffness and damping forces identified by response surface plot. A theoretical model $m\ddot{x} + n_k(x) + n_c(\dot{x}) = f(t)$ is used for predicting. The modeling contains linear and nonlinear stiffness and damping. The measured responses and the calculated ones are compared in Fig. 16. It can be seen that the identified mathematical model reveals the softening stiffness and the hardening damping well. It shows that it has the ability to identify system with certain ideal accuracy for a given excitation. Prediction should be within the range of the force levels. A broader range of excitation values is not recommended because the nonlinearity is not a specifical function with smooth property.

4 Conclusion

Nonlinearities in structural dynamics are common in complex and real structures. The response surface plot is proposed for identification and quantification of nonlinearity, which can be calculated by resulted FRFs and excitation level. In this procedure, vibration response data are obtained by normal vibration test and plotted as discrete points of vibration response, which is called as response surface plot. The response surface plot can be regarded as the displacement response over excitation and frequency, and the shift of resonant frequency and amplitude change can be observed by the resulted response surface plot. The equivalent stiffness and damping is obtained corresponding to resonant response amplitude. By fitting the equivalent stiffness and damping with suitable basis functions, the parameters or mathematical model with the unknown element can be identified by HBM. The procedure of response surface plot is validated by several classical nonlinear numerical cases and experimental application for its effectiveness and accuracy. This technique is simple and practical, which can deal with some nonlinearity with distorted FRF, such as jump. It is hopeful that this technique can be applied to some real structures and help engineer to characterize its nonlinear property without complex equipment and instrument.

References

[1] NOËL J P, KERSCHEN G. Nonlinear system identification in structural dynamics: 10 more years of progress [J]. *Mechanical Systems and Signal Processing*, 2017, **83**: 2-35.

[2] LIU X, SUN B B, LI L, et al. Nonlinear identification and characterization of structural joints based on vibration transmissibility [J]. *Journal of Southeast University* (*English Edition*), 2018, **34**(1): 36-42.

[3] CHEN C Y, SONG H W, WANG D Y, et al. The natural frequency shift of satellite vibration test and parameter identification of nonlinear in satellite structure [J]. *Journal of Shanghai Jiao Tong University*, 2005, **39**(7): 1197-1200 (in Chinese).

[4] AGUIRRE L A, LETELLIER C. Modeling nonlinear dynamics and chaos: A review [J]. *Mathematical Problems in Engineering*, 2009, **2009**: 238960.

[5] LIU X, WANG L X, CHEN Q D, et al. Nonlinear modeling and identification of structural joint by response control vibration test [J]. *Transactions of Nanjing University of Aeronautics and Astronautics*, 2019, **36**(6): 964-976.

[6] MAO K, LI B, WU J, et al. Stiffness influential factors-based dynamic modeling and its parameter identification method of fixed joints in machine tools [J]. *International Journal of Machine Tools and Manufacture*, 2010, **50**(2): 156-164.

[7] GÖGE D, SINAPIUS M, FÜLLEKRUG U, et al. Detection and description of non-linear phenomena in experimental modal analysis via linearity plots [J]. *International Journal of Non-Linear Mechanics*, 2005, **40**(1): 27-48.

[8] AHMADIAN H, ZAMANI A. Identification of nonlinear boundary effects using nonlinear normal modes [J]. *Mechanical Systems and Signal Processing*, 2009, **23**(6): 2008-2018.

[9] PRAWIN J, RAMA MOHAN RAO A, LAKSHMI K. Nonlinear identification of structures using ambient vibration data [J]. *Computers & Structures*, 2015, **154**: 116-134.

[10] NOËL J P, KERSCHEN G, FOLTÊTE E, et al. Grey-box identification of a non-linear solar array structure using cubic splines [J]. *International Journal of Non-Linear Mechanics*, 2014, **67**: 106-119.

[11] ALEJO D, ISIDRO L, JESÚS R, et al. Parameter estimation of linear and nonlinear systems based on orthogonal series [J]. *Procedia Engineering*, 2012, **35**: 67-76.

[12] GÖGE D, SINAPIUS M, FÜLLEKRUG U, et al. Detection and description of non-linear phenomena in experimental modal analysis via linearity plots [J]. *International Journal of Non-Linear Mechanics*, 2005, **40**(1): 27-48.

[13] SADATI S M S, NOBARI A S, NARAGHI T. Identification of a nonlinear joint in an elastic structure using optimum equivalent linear frequency response function [J]. *Acta Mechanica*, 2012, **223**: 1507-1516.

[14] ÖZER M B, ÖZGÜVEN H N, ROYSTON T J. Identification of structural non-linearities using describing functions and the Sherman-Morrison method [J]. *Mechanical Systems and Signal Processing*, 2009, **23**(1): 30-44.

[15] FELDMAN M, BRAUN S. Nonlinear vibrating system identification via Hilbert decomposition [J]. *Mechanical Systems and Signal Processing*, 2017, **84**: 65-96.

[16] JALALI H, AHMADIAN H, MOTTERSHEAD J E. Identification of nonlinear bolted lap-joint parameters by force-state mapping [J]. *International Journal of Solids and Structures*, 2007, **44**(25/26): 8087-8105.

[17] THOTHADRI M, CASAS R A, MOON F C, et al. Nonlinear system identification of multi-degree-of-freedom systems [J]. *Nonlinear Dynamics*, 2003, **32**(3): 307-322.

[18] AHMADIAN H, JALALI H. Generic element formulation for modelling bolted lap joints [J]. *Mechanical Systems and Signal Processing*, 2007, **21**(5): 2318-2334.

[19] ARSLAN Ö, AYKAN M, NEVZAT ÖZGÜVEN H. Parametric identification of structural nonlinearities from measured frequency response data [J]. *Mechanical Systems and Signal Processing*, 2011, **25**(4): 1112-1125.